第 40 卷 第 5 期
2025 年 10 月

新型炭材料（中英文）
New Carbon Materials

Cite this: New Carbon Materials, 2025, 40(5): 1193-1200

Read Online

Data paper

A dataset for the structure and electrochemical performance of hard carbon as anodes for sodium-ion batteries

HOU Wei-yan[1,2,3,†], YI Zong-lin[1,2,†], JIA Wan-ru[1,2,3], YU Hong-tao[1,2,3], DAI Li-qin[1,2], YANG Jun-jie[1,2], CHEN Jing-peng[1,2], XIE Li-jing[1,2,*], SU Fang-yuan[1,2,*], CHEN Cheng-meng[1,2,4,*]

(1. *Shanxi Key Laboratory of Carbon Materials*, *Institute of Coal Chemistry*, *Chinese Academy of Sciences*, *Taiyuan* 030001, *China*;

2. *CAS Key Laboratory of Carbon Materials*, *Institute of Coal Chemistry*, *Chinese Academy of Sciences*, *Taiyuan* 030001, *China*;

3. *University of Chinese Academy of Sciences*, *Beijing* 100049, *China*;

4. *Center of Materials Science and Optoelectronics Engineering*, *University of Chinese Academy of Sciences*, *Beijing* 100049, *China*)

Abstract: This data set collects, compares and contrasts the capacities and structures of a series of hard carbon materials, and then searches for correlations between structure and electrochemical performance. The capacity data of the hard carbons were obtained by charge/discharge tests and the materials were characterized by XRD, gas adsorption, true density tests and SAXS. In particular, the fitting of SAXS gave a series of structural parameters which showed good characterization. The related test details are given with the structural data of the hard carbons and the electrochemical performance of the sodium-ion batteries.

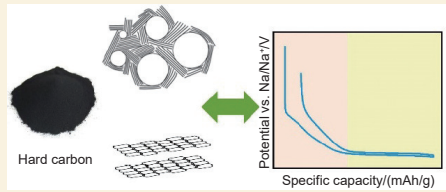

Key words: Hard carbon; Sodium-ion battery; SAXS; Structural characterization; Dataset

Specifications table

Subject	Material
Specific subject area	Sodium-ion batteries
Type of data	Table and image
How data was acquired	The discharge and charge tests were conducted using the LAND CT2001 battery tester (LAND, Wuhan, China) within a voltage range of 0–2 V. X-ray Diffraction (XRD, D8 Advance, Bruker, Germany) was employed to characterize the microcrystalline structures of HCs. Pore structure analysis was performed using CO_2 and N_2 as adsorbents on a Micromeritics TriStar II 3020 and BELSOPR-max II analyzers, respectively. The true density (AccuPyc II 1340, America) was performed using helium as analysis gas and the closed pore volume was calculated by true density. Further information of pore structure was obtained by small-angle X-ray scattering (SAXS, Xenocs Xeuss 2.0, French).
Data format	Raw and analyzed
Experimental factors	Samples, assembled coin cells metallic sodium foil as cathodes and fitting process.
Experimental features	Capacity performance of discharge and charge, structural character and SAXS fitting results.
Data source location	CAS Key Laboratory of Carbon Materials, Institute of Coal Chemistry, Chinese Academy of Sciences, Taiyuan, China
Data accessibility	The data is with the article and available from the URL: https://www.scidb.cn/detail?dataSetId=7e7687dfcf9042ec91d36c33dcfcc992.

Value of the data

- Detailed electrochemical performance and structural characterization data might be used for further studies.
- SAXS fitting method and result data can be used for more scientific analysis of microstructure of the closed pore and carbon layers of hard carbon materials.
- Electrochemical performance and structure data of hard carbon materials can be utilized to compare together and used for the optimization of material design.

Data description

In this data article, the detailed electrochemical performance and structural characterization data of the hard carbon materials are presented. The data include the electrochemical capacity performance (Fig. 1, raw data in Table 1), the structure characterization data (Table 2), capacity performance data of hard carbon anodes obtained from other literatures (Table 3) and the SAXS fitting result data (Table 4). In addition, a series of structure-performance correlations are summarized.

Received: February 03, 2025
Revised: June 09, 2025
Accepted: June 10, 2025
DOI: 10.1016/S1872-5805(25)61004-3
CSTR: 32158.14.S1872-5805(25)61004-3

Table 1 Electrochemical discharge capacity performance of hard carbon materials

sample	ICE/%	Capacity/mAh g^{-1}	Slope capacity/(mAh g^{-1})	Percentage of slope capacity/%	Plateau capacity/(mAh g^{-1})	Percentage of plateau capacity/%
HC-1	91.20	304.6	95.5	31.4	209.1	68.6
HC-2	91.24	297.3	95.7	32.2	201.6	67.8
HC-3	88.62	284.3	79.0	27.8	205.3	72.2
HC-4	88.41	315.3	63.7	20.2	251.6	79.8
HC-5	83.58	250.8	123.7	49.3	127.1	50.7
HC-6	83.09	250.4	95.7	38.2	154.1	61.8
HC-7	90.90	295.7	59.7	20.2	236.0	79.8
HC-8	89.84	285.8	77.7	27.2	208.1	72.8
HC-9	–	–	–	–	–	–
HC-10	87.06	287.3	76.0	26.4	211.3	73.6
HC-11	90.93	319.8	67.3	21.1	252.4	78.9
HC-12	89.79	299.7	74.8	25.0	224.9	75.0
HC-13	89.87	337.8	71.7	21.2	266.1	78.8
HC-14	90.89	313	51.3	16.4	261.7	83.6
HC-15	88.99	285.9	74.0	25.9	211.9	74.1
HC-16	88.86	302.3	95.7	31.7	206.6	68.3
HC-17	91.67	308.8	72.0	23.3	236.9	76.7
HC-18	89.62	297.9	86.5	29.0	211.4	71.0
HC-19	89.88	307.7	78.2	25.4	229.5	74.6
HC-20	88.97	311.1	72.0	23.1	239.1	76.9
HC-21	87.08	292.8	75.0	25.6	217.8	74.4
HC-22	88.21	351.5	69.1	19.7	282.4	80.3
HC-23	87.50	296.1	84.0	28.4	212.1	71.6
HC-24	90.02	358.6	71.8	20.0	286.8	80.0
HC-25	89.34	338.5	76.0	22.5	262.5	77.5
HC-26	88.66	299.5	74.0	24.7	225.5	75.3
HC-27	–	–	–	–	–	–
HC-28	83.18	248.4	60.2	24.2	225.5	75.8
HC-29	88.21	328.5	80.0	24.3	248.5	75.7
HC-30	86.05	317.1	91.2	28.8	225.9	71.2
HC-31	84.37	257.6	82.0	31.8	175.6	68.2
HC-32	85.10	294.8	66.2	22.5	228.6	77.5
HC-33	85.98	295.8	88.5	29.9	207.3	70.1
HC-34	91.97	301.2	71.7	23.8	229.5	76.2
HC-35	90.60	305.9	73.0	23.9	232.9	76.1
HC-36	91.36	294.4	66.0	22.4	228.4	77.6
HC-37	90.69	288.1	66.3	23.0	221.8	77.0
HC-38	91.38	298.4	67.8	22.7	230.6	77.3
HC-39	86.59	279.6	62.5	22.4	217.1	77.6
HC-40	87.56	283.3	62.0	21.9	221.3	78.1
HC-41	–	–	–	–	–	–
HC-42	81.25	268.8	70.8	26.3	198	73.7
HC-43	91.59	302.7	66.2	21.9	236.5	78.1
HC-44	91.79	310.5	67.5	21.7	243.0	78.3
HC-45	89.70	299.2	69.2	23.1	230.0	76.9
HC-46	87.13	295.5	74.0	25.0	221.5	75.0
HC-47	86.68	267.7	107.7	40.2	160.0	59.8
HC-48	85.86	277.4	94.7	34.1	182.7	65.9
HC-56	87.00	346.8	86.6	24.9	260.2	75.1
HC-57	84.05	311.3	78.0	25.1	233.3	74.9
HC-61	89.49	401.8	72.0	17.9	329.8	82.1
HC-62	85.89	318.6	72.2	22.6	246.5	77.4

Table 2 Structure parameters of the hard carbon materials

Sample	d_{002} /Å	*Lc* /nm	*La* /nm	S_{BET} (N_2) /(m^2 g^{-1})	S_{BET} (CO_2) /(m^2 g^{-1})	True density /(g cm^{-3})	Closed pore volume /(cm^3 g^{-1})
HC-1	3.88	0.87	2.99	6.13	3.00	2.07	0.041
HC-2	3.8	1.41	2.18	5.04	6.15	2.07	0.041
HC-3	3.9	0.84	3.99	1.82	33.90	1.99	0.061
HC-4	3.8	0.83	4.07	3.24	107.54	1.96	0.068
HC-5	3.6	0.73	2.00	2.63	216.76	2.02	0.053
HC-6	3.9	0.82	4.25	12.48	117.64	1.91	0.081
HC-7	3.8	0.86	4.35	11.51	145.86	1.86	0.095
HC-8	3.9	0.82	2.96	4.06	10.18	1.96	0.068
HC-9	3.8	1.49	4.26	5.12	18.30	2.06	0.043
HC-10	3.8	0.91	3.89	6.04	46.65	2.04	0.048
HC-11	3.8	0.61	3.89	14.03	9.23	1.95	0.070
HC-12	3.8	0.59	4.86	10.97	9.34	2.03	0.051
HC-13	3.8	0.53	5.12	5.58	21.21	2.05	0.046
HC-14	3.8	0.66	4.31	2.03	49.83	2.02	0.053
HC-15	3.9	0.61	3.43	5.28	13.58	2.03	0.051
HC-16	3.9	1.33	4.86	7.52	13.94	2.06	0.044
HC-17	3.8	0.65	4.85	5.33	12.43	2.00	0.058
HC-18	3.8	0.69	4.01	8.39	13.92	2.06	0.043
HC-19	3.8	1.06	3.34	9.18	14.12	2.05	0.044
HC-20	–	–	–	6.27	4.16	–	–
HC-21	–	–	–	6.45	0.47	–	–
HC-22	–	–	–	6.69	24.44	–	–
HC-23	–	–	–	6.49	5.00	–	–
HC-24	3.9	–	–	–	–	–	–
HC-25	3.8	–	–	–	–	–	–
HC-26	3.8	0.64	3.99	6.42	16.95	2.07	0.042
HC-27	3.8	0.61	4.31	4.43	47.84	2.07	0.040
HC-28	3.6	0.57	4.26	8.82	9.34	1.91	0.082
HC-29	3.8	1.20	2.41	5.21	55.89	2.09	0.040
HC-30	3.9	0.59	4.08	9.98	429.43	2.16	0.020
HC-31	3.8	0.80	3.95	5.05	34.49	2.03	0.050
HC-32	3.8	0.58	3.90	21.61	21.05	1.76	0.124
HC-33	3.8	0.68	3.23	5.23	11.99	2.08	0.038
HC-56	3.8	0.90	4.14	–	569.20	–	
HC-57	3.8	0.90	4.18	–	82.00	–	0.124
HC-58	3.6	0.99	3.57	–	268.95	–	0.120
HC-59	3.7	1.03	3.65	–	229.92	–	
HC-60	3.9	0.99	3.81	–	353.06	–	0.073
HC-61	3.8	0.95	3.97	–	561.77	–	0.010
HC-62	3.7	0.94	4.11	–	555.23	–	0.042
HC-71	3.5	–	–	–	–	–	–
HC-72	3.8	–	–	–	–	–	–

Methods and experimental design

The electrodes were fabricated by applying a slurry of 93% (mass fraction, the same below) of active materials, 2% of Super P, 2% of carboxymethyl cellulose (CMC) and 3% of styrene-butadiene rubber (SBR) to copper foil current collector and then drying in a vacuum oven at 100 °C for 12 h to remove water totally. The average loading mass of active materials is 5 mg cm^{-2}. The CR2032 coin cells were assembled in a glove box (H_2O, O_2 < 0.1×10^{-6}) with the electrodes, counter-electrodes (sodium metal), separators (glass fibers) and electrolyte (1.0 mol L^{-1} $NaPF_6$ in EC/DEC = 1 : 1, weight). The Galvanostatic discharge and charge tests were conducted using the LAND CT2001 battery tester (LAND, Wuhan, China) within a voltage range of 0–2 V at approximately 25 °C. The discharge process was carried out by means of multiple discharges at small currents, in order to ensure complete sodiation of the hard carbon by repeated discharges to 0 V at 0.2 C, 0.15 C, 0.12 C, 0.08 C, 0.06 C, 0.05 C, 0.04 C, 0.03 C, 0.02 C, 0.015 C, 0.012 C, 0.01 C, 20 μA and 10 μA in turn. Charge to 2 V at 0.1 C.

The statistics of the capacity performance are presented in Fig. 1. As shown in Fig.1a, the total capacity of hard carbons are concentrated around 300 mAh g^{-1}, which are mainly contributed by the plateau capacity. In addition, the slope capacity is less than 100 mAh g^{-1}, and the distribution is more concentrated than plateau capacity. We compared the electrochemical performance of commercial hard carbon with that of the hard carbon in the latest article, and found that the capacity and ICE are in the same range. The percentages of capacity are shown in Fig. 1b, in which we can conclude that the main contribution of capacity is plateau capacity, which is concentrated around 80%. And several types of hard carbon have a percentage of slope capacity more than 50%, which means a greater kinetic performance.

The SAXS curves were fitted with Origin 2025. First, import the .dat file of the SAXS results into the Origin Sheet, and then select the scattering vector and the mean scattering cross section as X and Y for scatter plots, respectively. Then, convert the X, Y-axis to log-log scale and the scatter plots will show a shoulder-like peak in the mid-angle region (Fig. 2a). As shown in Fig. 2a, the fitting process can be consisted of 2 parts. The one is the shoulder-like peak fitted using the Teubner-Strey model developed by Damien Saurel et al, from which a series of structural parameters are revealed like d (pore-pore distance), r (average pore diameter), f_a (pore connectivity) and ξ (correlation length that limits the extension of the order)[6]. The other is the linear-part at the end of the shoulder-like peak, and the absolute value of the slope is D (fractal dimension), which is related to the degree of bending of the carbon layer[7]. The detailed SAXS fitting parameters are displayed in Table 4.

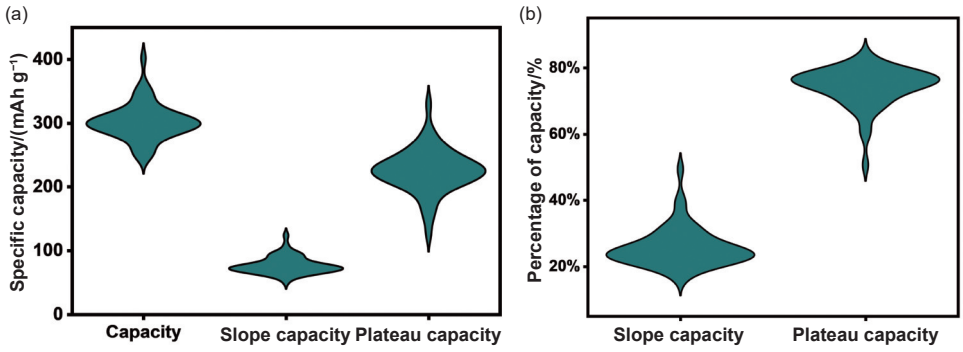

Fig. 1 (a) The statistical results of total capacity, slope capacity and plateau capacity. (b) The percentage of slope capacity and plateau capacity

Table 3 Comparison of electrochemical properties of hard carbon with the latest literature

Sample	Current density/(A/g)	Capacity/(mAh/g)	ICE/%
HC-N[1]	0.02	356.0	88.1
HC-P[1]	0.02	266.0	83.5
	0.02	320.0	—
HCK-1[2]	0.05	303.0	—
	0.10	285.0	80.4
HCK-0.5[2]	0.10	235.1	77.2
HCK-2[2]	0.10	272.6	77.7
HC-NB[3]	0.02	301.2	86.6
HC-DB-6[3]	0.02	350.0	86.8
HC-DB-12[3]	0.02	288.9	86.1
HC-220[4]	0.03	190.0(plateau)	—
HC-300[4]	0.03	230.0(plateau)	—
HC-320[4]	0.03	210.0(plateau)	—
PP-1400[5]	0.03	274.7	85.4
TS-1400[5]	0.03	261.6	84.7
THFS-1400[5]	0.03	296.8	86.8
THFI-1400[5]	0.03	309.7	91.0

Table 4 SAXS fitting results of the hard carbon materials

Sample	d/nm	ξ/nm	f_a-	r/nm	D/
HC-1	4.00	0.37	0.50	0.71	2.34
HC-2	3.89	0.38	0.45	0.69	2.38
HC-3	4.42	0.47	0.39	0.77	2.56
HC-4	4.02	0.53	0.19	0.56	2.68
HC-5	—	0.18	2.35	1.13	2.00
HC-6	4.65	0.47	0.42	0.82	2.66
HC-7	4.26	0.48	0.33	0.71	2.62
HC-8	4.48	0.42	0.48	0.80	2.61
HC-9	4.46	0.45	0.43	0.79	2.53
HC-10	4.58	0.47	0.40	0.80	2.61
HC-11	4.00	0.48	0.28	0.64	2.64
HC-12	4.61	0.47	0.42	0.81	2.60
HC-13	4.03	0.50	0.24	0.61	2.71
HC-14	4.50	0.49	0.37	0.77	2.72
HC-15	4.13	0.48	0.31	0.68	2.53
HC-16	4.12	0.48	0.31	0.68	2.50
HC-17	4.02	0.53	0.18	0.55	2.64
HC-18	4.73	0.42	0.53	0.84	2.47
HC-19	4.30	0.47	0.36	0.74	2.59
HC-20	—	—	—	—	—
HC-21	—	—	—	—	—
HC-22	—	—	—	—	2.72
HC-23	—	—	—	—	—
HC-24	3.76	0.53	0.12	0.43	2.72
HC-25	4.31	0.57	0.19	0.60	2.74
HC-26	—	—	—	—	2.6
HC-27	—	—	—	—	2.64
HC-28	—	—	—	—	1.94
HC-29	3.88	0.49	0.23	0.58	2.64
HC-30	3.46	0.48	0.13	0.42	2.52
HC-31	—	0.34	1.75	1.66	2.49
HC-32	5.15	0.52	0.42	0.91	2.77
HC-33	—	—	—	—	2.42
HC-34	3.93	0.49	0.23	0.59	2.65
HC-35	5.09	0.45	0.53	0.90	2.61
HC-36	5.67	0.43	0.63	0.98	2.63
HC-37	—	—	—	—	2.6
HC-38	—	—	—	—	2.63
HC-39	5.31	0.47	0.52	0.94	2.64
HC-40	5.07	0.47	0.49	0.90	2.61
HC-41	5.19	0.45	0.54	0.92	2.58
HC-42	5.25	—	0.56	0.93	2.51
HC-43	4.24	0.45	0.39	0.74	2.59
HC-44	4.30	0.46	0.37	0.74	2.62
HC-45	—	—	—	—	2.68
HC-46	—	—	—	—	2.59
HC-47	—	—	—	—	2.25
HC-48	—	—	—	—	2.54
HC-49	4.01	0.48	0.27	0.64	2.64
HC-50	4.12	0.45	0.36	0.70	2.62
HC-51	4.37	0.44	0.43	0.77	2.63
HC-52	4.39	0.45	0.42	0.77	2.65
HC-53	5.49	0.41	0.64	0.94	2.59
HC-54	—	—	—	—	2.61
HC-55	—	—	—	—	2.36
HC-56	3.45	0.54	0.01	0.14	2.74
HC-57	5.87	0.39	0.71	0.95	2.55
HC-58	9.92	0.37	0.90	7.07	2.52
HC-59	8.49	—	0.87	1.01	2.02
HC-60	6.87	0.48	0.68	1.14	2.72
HC-61	6.82	0.50	0.64	1.16	2.78
HC-62	8.99	—	0.92	0.89	2.21
HC-63	4.54	0.51	0.34	0.77	2.66
HC-64	3.99	0.52	0.20	0.57	2.57
HC-65	4.92	0.42	0.55	0.87	2.50

The statistical distributions of the parameters obtained from the SAXS curve fitting are presented in Fig. 2b-f. We can learn from these figures that the microstructure of hard carbons is characterized by the fact that these parameters are not randomly distributed, they are concentrated in a certain range instead. The distributions of ξ and D are similar, they are concentrated between 0.4-0.5 and 2.5-2.7, respectively. And there are a few types of hard carbon concentrate independently, where a D value is around 2, and their XRD parameters show soft carbon nature[8].

We attempted to systematically correlate the electrochemical performances with the interlayer distance of hard carbon by determining the R^2 coefficient. The electrochemical performance evolution is represented as a function of d_{002} and the obtained data are fitted with a linear function, which give the determination factor R^2. The detailed fitted data are presented in Fig. 3a-e, while Fig. 3f gathers the R^2 values for all electrochemical performance parameters. It is clear that none of the correlations between d_{002} and electrochemical performances are strong. Among them, the slope capacity, the plateau capacity and the percentage of capacities have a low correlation with the interlayer distance. In addition, it can be seen that the percentage of plateau capacity increases with d_{002}, while the slope capacity and plateau capacity show opposite correlations. It may originate from the fact that a larger d_{002} provides a higher insertion capacity which result in a higher slope capacity, while a smaller d_{002} implies a more regular internal structure and less closed pores, resulting in a lower plateau capacity. It is worth noting that we can only draw this conclusion from the difference in trends, but the very low correlation suggests that d_{002} is not a decisive influence on the capacity of the hard carbon anode. In fact, the d_{002} peak of hard carbon broadens rather than a spike due to defects, cross-linked structures and closed pores, which results in an average interlayer distance for hard carbon materials, which may contain variations in interlayer distance due to the various disordered structures mentioned above.

Further, we analyzed the correlation of the closed-hole pore volume and small-angle X-ray scattering fitting parameters with the plateau capacity and found some stronger correlations than d_{002}. As shown in Fig.4a and Fig.4b, the closed pore volume and d have weak correlations with plateau capacity. Meanwhile, the plateau capacity decreases with r in Fig. 4c. It is interesting that with the increase of d_{002} and average pore diameter, the plateau capacity decrease. Therefore, we believe that the mere size of the sodium storage space is not a determining factor for plateau capacity. As shown in Fig.4d-f, f_a, ξ and D show

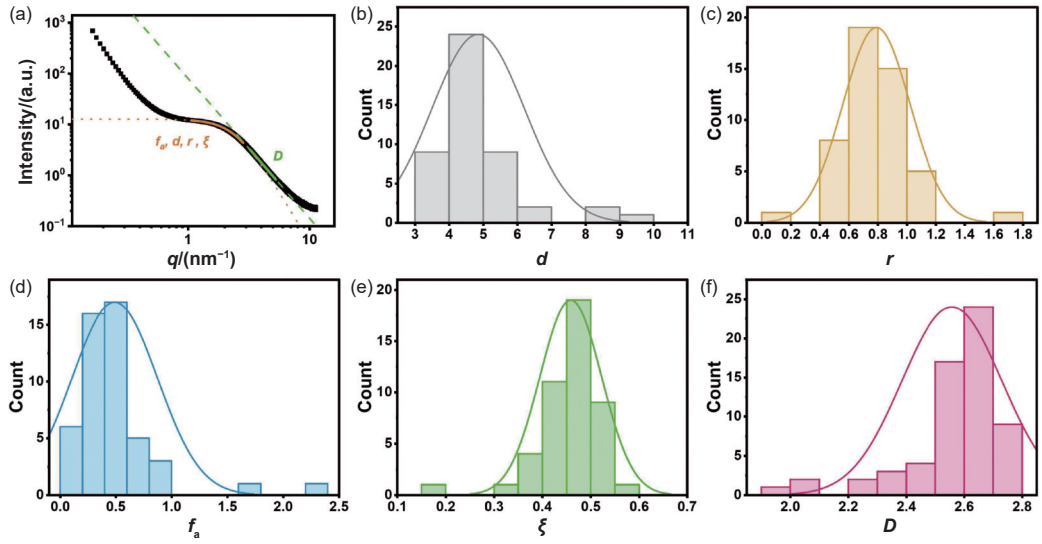

Fig. 2 (a) Schematic of the SAXS curve fitting. (b-f) Statistical distribution of SAXS curve fitting results: (b) d (pore-pore distance), (c) r (average pore diameter), (d) f_a (pore connectivity), (e) ξ (correlation length that limits the extension of the order) and (f) D (fractal dimension)

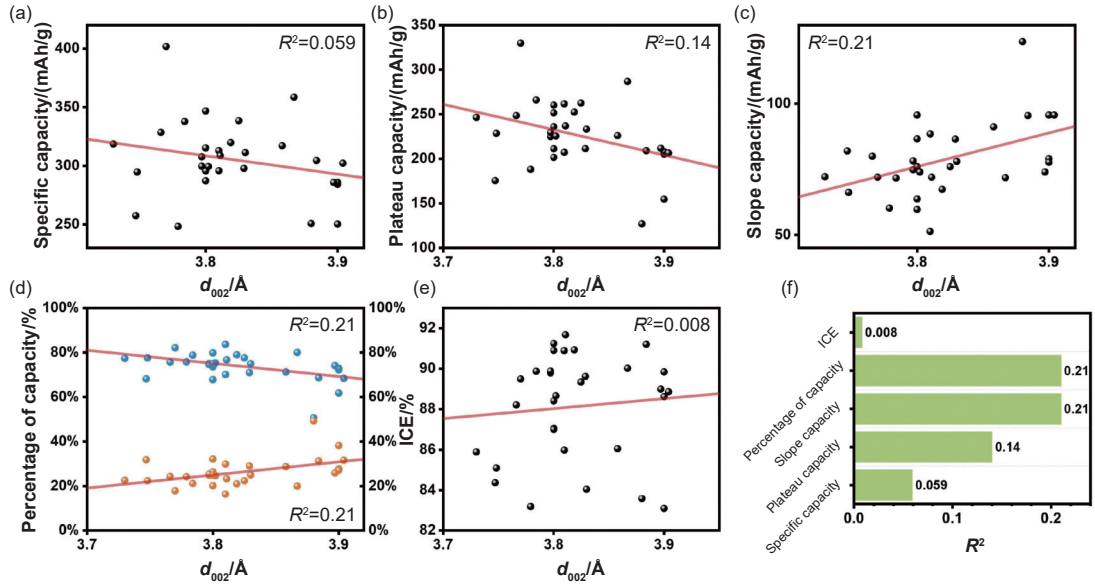

Fig. 3 The relationship among interlayer distance of hard carbon and different electrochemical performances. (a) Specific capacity. (b) Plateau capacity. (c) Slope capacity. (d) Percentage of capacities (blue plots: plateau capacity, orange plots: slope capacity). (e) Initial Coulombic Efficiency (ICE). (f) Interlayer distance correlations with electrochemical performances given by R^2 coefficient of determination

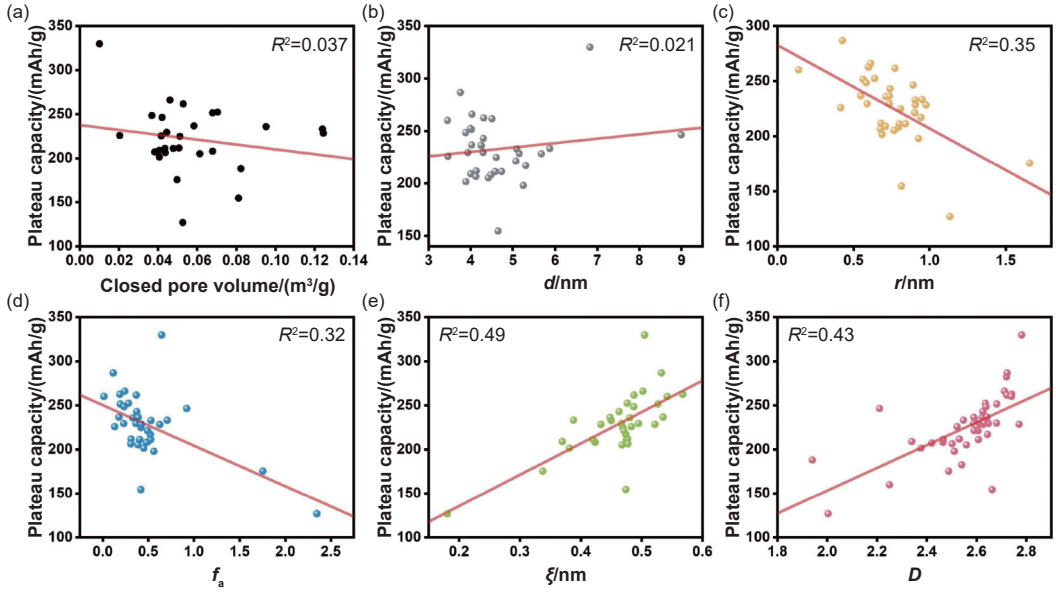

Fig. 4 Relationship among plateau capacity and structural parameters. (a) Closed pore volume. (b-f) d, r, f_a, ξ and D fitting from SAXS curve

stronger correlations with plateau capacity and the plateau capacity is negatively correlated with f_a and positively correlated with ξ and D. Obviously, the average pore diameter increases as the pore connectivity increases, since multiple pores connected will form a larger pore. Meanwhile, the increase of ξ and D means the increase in the degree of disorder in the hard carbon structure, which would provide more sodium storage sites and lead to a larger plateau capacity.

Acknowledgements

This work was supported by the National Natural Science Foundation of China (22379157), CAS Project for Young Scientists in Basic Research (YSBR-102); Institute of Coal Chemistry, Chinese Academy of Sciences (SCJC-XCL-2023-13, SCJCX-CL-2023-10), Talent Projects for Outstanding Doctoral Students to Work in Shanxi Province (E3SWR4791Z) and Fundamental Research Program

of Shanxi Province (202403021222485).

Author information

***Corresponding authors:**

XIE Li-jing, Associate Professor. E-mail: chencm@sxicc.ac.cn;

SU Fang-yuan, Professor. E-mail: Sufangyuan@sxicc.ac.cn;

CHEN Cheng-meng, Professor. E-mail: Xielijing@sxicc.ac.cn

First author:

†HOU Wei-yan and †YI Zong-lin contributed equally to this work.

References

[1] Huang Y, Hou Z, Wang J, et al. Reconfiguring terminal species of bituminous coal to steer hard carbon toward high - capacity and fast sodium storage[J]. Angewandte Chemie International Edition, 2025, 64(15).

[2] Hou Z, Jiang M, Lei D, et al. Regulation of pseudographitic carbon domain to boost sodium energy storage[J]. Nano Research, 2024, 17(6): 5188-5196.

[3] Wang Y, Yi Z, Xie L, et al. Releasing free radicals in precursor triggers the formation of closed pores in hard carbon for sodium-ion batteries[J]. Advanced Materials, 2024, 36(26): 2401249.

[4] Mao Y, Yi Z, Xie L, et al. Elimination of hydrogen bonds in cellulose enables high-performance disordered carbon anode in sodium-ion batteries[J]. Energy Storage Materials, 2024, 73: 103845.

[5] Zhang X, Yi Z, Tian Y, et al. Insight into the effect of structural differences among pitch fractions on sodium storage performance of pitch-derived hard carbons[J]. Carbon, 2024, 226: 119165.

[6] Saurel D, Segalini J, Jauregui M, et al. A saxs outlook on disordered carbonaceous materials for electrochemical energy storage[J]. Energy Storage Materials, 2019, 21: 162-173.

[7] Hou W, Yi Z, Yu H, et al. Fractal dimension revealed from saxs as a descriptor of structural disorder in hard carbon anodes of sodium ion battery[J]. Chinese Chemical Letters, 2025: 111124.

[8] Mu B Y, Chi C L, Yang X H, et al. A review of hard carbon anodes for rechargeable sodium-ion batteries[J]. New Carbon Materials, 2024, 39(5): 796-823.

钠离子电池硬炭负极的微观结构与其电化学性能数据集

侯玮琰[1,2,3,†]，易宗琳[1,2,†]，贾惋茹[1,2,3]，余洪涛[1,2,3]，戴丽琴[1,2]，杨俊杰[1,2]，陈景鹏[1,2]，谢莉婧[1,2,*]，苏方远[1,2,*]，陈成猛[1,2,4,*]

（1. 中国科学院山西煤炭化学研究所，炭材料山西重点实验室，太原 030001；
2. 中国科学院炭材料重点实验室，中国科学院山西煤炭化学研究所，太原 030001；
3. 中国科学院大学，北京 100049；
4. 中国科学院大学材料科学与光电工程中心，北京 100049）

摘　要： 本数据集的目的是收集、比较并分析一系列硬炭材料的容量与结构数据，进而探究其结构与电化学性能之间的关联。我们通过充放电测试获取了硬炭的容量数据，并利用 X 射线衍射（XRD）、气体吸附、真密度测试和小角 X 射线散射（SAXS）等手段对其结构进行了表征。其中，通过 SAXS 曲线拟合获得了一系列具有良好结构表征能力的参数。本文详细描述了结构测试细节，并提供了硬炭材料的结构数据及其在钠离子电池中的电化学性能。

关键词： 硬炭；钠离子电池；SAXS；结构表征；数据集

中图分类号： 127.1+1　　**文献标识码：** A

通讯作者：谢莉婧. E-mail: chencm@sxicc.ac.cn;
苏方远. E-mail: Sufangyuan@sxicc.ac.cn;
陈成猛. E-mail: Xielijing@sxicc.ac.cn

第一作者：†侯玮琰和†易宗琳为共同第一作者.

本文的电子版全文由 Elsevier 出版社在 ScienceDirect 上出版（https://www.sciencedirect.com/journal/new-carbon-materials/）